ORIGINAL PAPER

Free fatty acid receptor 4 activation protects against choroidal neovascularization in mice

Yohei Tomita[1] · Bertan Cakir[1] · Chi-Hsiu Liu[1] · Zhongjie Fu[1] · Shuo Huang[1] · Steve S. Cho[1] · William R. Britton[1] · Ye Sun[1] · Mark Puder[2] · Ann Hellström[3] · Saswata Talukdar[4] · Lois E. H. Smith[1]

Abstract

To examine whether free fatty acid receptor 4 (FFAR4) activation can protect against choroidal neovascularization (CNV), which is a common cause of blindness, and to elucidate the mechanism underlying the inhibition, we used the mouse model of laser-induced CNV to mimic angiogenic aspects of age-related macular degeneration (AMD). Laser-induced CNV was compared between groups treated with an FFAR4 agonist or vehicle, and between FFAR4 wild-type ($Ffar4^{+/+}$) and knock out ($Ffar4^{-/-}$) mice on a C57BL/6J/6N background. The ex vivo choroid-sprouting assay, including primary retinal pigment epithelium (RPE) and choroid, without retina was used to investigate whether FFAR4 affects choroidal angiogenesis. Western blotting for pNF-κB/NF-κB and qRT-PCR for $Il-6, Il-1β, Tnf-α, Vegf,$ and $Nf-κb$ were used to examine the influence of FFAR4 on inflammation, known to influence CNV. RPE isolated from $Ffar4^{+/+}$ and $Ffar4^{-/-}$ mice were used to assess RPE contribution to inflammation. The FFAR4 agonist suppressed laser-induced CNV in C57BL/6J mice, and CNV increased in $Ffar4^{-/-}$ compared to $Ffar4^{+/+}$ mice. We showed that the FFAR4 agonist acted through the FFAR4 receptor. The FFAR4 agonist suppressed mRNA expression of inflammation markers ($Il-6, Il-1β$) via the NF-κB pathway in the retina, choroid, RPE complex. The FFAR4 agonist suppressed neovascularization in the choroid-sprouting ex vivo assay and FFAR4 deficiency exacerbated sprouting. Inflammation markers were increased in primary RPE cells of $Ffar4^{-/-}$ mice compared with $Ffar4^{+/+}$ RPE. In this mouse model, the FFAR4 agonist suppressed CNV, suggesting FFAR4 to be a new molecular target to reduce pathological angiogenesis in CNV.

Introduction

Age-related macular degeneration (AMD) is a leading cause of vision loss in industrialized nations. Almost two-thirds of the population over 80 years of age has signs of AMD, which is characterized initially by the presence of drusen.

✉ Lois E. H. Smith
Lois.Smith@childrens.harvard.edu

1 Department of Ophthalmology, Boston Children's Hospital, Harvard Medical School, 300 Longwood Ave, Boston, MA 02115, USA

2 Vascular Biology Program and Department of Surgery, Boston Children's Hospital, Boston, USA

3 Pediatric Ophthalmology, Sahlgrenska Academy, The Queen Silvia Children's Hospital, Göteborg, Sweden

4 Merck & Co., Inc., South San Francisco, CA, USA

Later stages may progress to neovascular AMD, particularly choroidal neovascularization (CNV) [1, 2]. Anti-VEGF therapy is not always effective in treating CNV. Because it is injected up to once per month it carries cumulative risks of infection and geographic atrophy [3–5]. The number of people with AMD is predicted to rise to 196 million in 2020 and 288 million in 2040, thus effective alternative treatments are urgently needed [6].

Experimentally, laser-induced CNV model aspects of CNV are seen in neovascular AMD [7]. This model uses photocoagulation to disrupt Bruch's membrane, inducing the growth of new choroidal vessels (CNV) into the subretinal area [8]. We previously optimized details of the laser-induced CNV model using an image-guided laser photocoagulation system [9]. This model has provided preclinical evidence to support the clinical evaluation of anti-VEGF drugs for ocular neovascular diseases [10].

The pathogenesis of neovascular AMD is incompletely understood but inflammation is thought to be a potent initiator of angiogenesis [11]. An important hallmark of AMD is the accumulation of lipid debris under the retinal pigment epithelium [12]. During aging, lipid metabolites, are processed and deposited under retinal pigment epithelial (RPE) cells and may cause chronic inflammation initiating AMD [13, 14]. Therefore, it is important to consider the regulation of lipid metabolism and inflammation when addressing this disease.

Our prior work showed that increased dietary intake of omega-3-polyunsaturated fatty acids (PUFAs) reduces pathological retinal angiogenesis in an animal model [15]. In addition, we have shown that free fatty acid receptor (FFAR)1, which binds omega-3 PUFA, is involved in the pathogenesis of neovascularization seen in very low-density lipoproteins receptor (VLDLR) deficient mice [16].

Another free fatty acid receptor, FFAR4, also known as G-protein coupled receptor 120 (GPR120), is expressed in retina as well as in hypothalamus, taste buds, liver, intestine, pancreas, adipose tissue, macrophages [16–18]. FFAR4 is linked to the regulation of body weight, inflammation, insulin resistance, and obesity [17, 19]. Omega-3 long chain polyunsaturated fatty acids inhibit inflammation and enhance systemic insulin sensitivity in mice with a high-fat diet, but these effects are abolished in FFAR4 knockout (KO) ($Ffar4^{-/-}$) mice [20]. FFAR4 has a key role in sensing dietary fat and controls energy balance in both humans and rodents [19]. FFAR4 also plays a role in the lipid-sensing cascade of ghrelin-expressing cells, to regulate energy and glucose homeostasis [21]. A FFAR4 selective agonist improves insulin resistance and chronic inflammation [22].

However, the relationship between FFAR4 and CNV has not been explored. In this study, we investigated whether FFAR4 influenced CNV and explored the mechanism.

Materials and methods

Animal

Male C57BL/6J mice were purchased from Jackson Laboratory. FFAR4 knockout mice ($Ffar4^{-/-}$, C57BL/6N/6J background) were purchased from UC Davis. All animals were housed with a 12-h light/ dark cycle. The animals were anesthetized with ketamine hydrochloride and xylazine hydrochloride. To dilate mouse pupils, Cyclomydril (AX10094, Alcon Laboratories, Inc., Fort Worth, TX, USA) was topically used.

Laser-induced CNV and drug treatment

CNV was induced in mice with laser as previously described [9, 23]. Six- to eight-week-old C57BL/6J (wild-type; WT) and $Ffar4^{-/-}$ mice were anesthetized with ketamine and xylazine. A green argon laser (an incident power of 240 mW and pulse duration of 70 ms) with Micron IV imaging-guiding system (Phoenix Research Laboratories, Pleasanton, CA, USA) was used to produce laser burns applied to 4 areas of the fundus of each eye. After laser photocoagulation, FFAR4 agonist (CpdA, Merck & Co., Inc., South San Francisco, CA, USA) [22] or vehicle control (Dimethyl Sulfoxide 10%, Polyethylene glycol 30%, distilled water 60%) were injected intraperitoneally (i.p.) or intravitreally to C57BL/6J or $Ffar4^{-/-}$ mice. Eyes were enucleated and fixed in 4% paraformaldehyde (PFA) for 1 h at room temperature. The choroid was permeabilized with 1% Triton X-100 PBS for 30 min at room temperature and stained overnight with fluorescent Griffonia Bandeiraea Simplicifolia Isolectin B4 (Alexa Fluor 594, I21413, Molecular Probes, Grand Island, NY, USA; 10 µg/mL) in 1 mM CaCl2 in 1% Triton X-100 PBS. The choroid was washed with PBS, whole mounted and photographed on a ZEISS Axio Observer Z1 microscope (ZEISS, Oberkochen, Germany). Lesion area was measured, and exclusion criteria were followed per previous publications [9].

Fundus fluorescein angiography (FFA)

Mice were injected intraperitoneally with fluorescein AK-FLUOR® (NDC 17478-101-12, Akorn, Lake Forest, IL, USA) at 10 µg/g body weight under anesthesia with ketamine and xylazine at 6 days after laser photocoagulation. Mouse pupils were dilated with Cyclomydril and fundus images of fluorescence were taken with a retinal-imaging system (Micron IV; Phoenix Research Laboratories, Pleasanton, CA, USA) at 5 and 10 min after injection. We analyzed the integrated intensity of fluorescence as an indicator of vascular leakage and subtracted 5 min readings from 10 min readings using ImageJ.

Primary RPE isolation and quantitative real-time RT-PCR

Quantitative real-Time PCR was performed as previously described [23]. Freshly isolated retina, choroid, and RPE complex were lysed with QIAzol lysis reagent and incubated on ice for 15 min, and 20% chloroform was added. Mixtures were incubated for 5 min at room temperature. Primary RPE was also isolated from choroid RPE complex in 7-month-old C57BL/6J mice using RNAprotect® cell reagent (#76526;

QIAGEN, Hilden, Germany) as previously reported [24]. The mixture was centrifuged at 12,000×g for 15 min, and the supernatant was collected for RNA extraction according to the manufacturer's instructions using a PureLink RNA Mini Kit (#12183018A; Invitrogen, Grand Island, NY, USA). RNA was then reverse transcribed using iScript cDNA synthesis kit (#1708891; BioRad, Hercules, CA, USA). Gene expression (mRNA) was quantified using an Applied Biosystems 7300 Real-Time PCR system (Thermo Fisher Schientific, Waltham, MA, U.S.A) with SYBR Green Master mix kit (bimake.com, Houston, TX, USA). Gene expression was calculated relative to 18S internal control for mouse retina, choroid, RPE complex using the $\Delta \Delta C_t$ method. The relative mRNA levels are presented as the ratio of change versus internal control (*Gapdh*). Oligonucleotide primers are listed in Table 1.

Western blotting

Choroidal-retinal explants were homogenized and protein was extracted in radio immunoprecipitation assay buffer (RIPA) (#89900; Pierce, Grand Island, NY, USA) supplemented with phosphatase inhibitor (1:100, #P0044, Sigma-Aldrich Corp., St. Louis, MO, USA) and protease inhibitor (1:100, #P8340, Sigma-Aldrich Corp.) and left overnight at 4 °C, Forty micrograms protein lysate was used to detect the levels of phosphorylated NF-κB p65 (pNF-κB, 1:500, #3033; Cell Signaling, Beverly, MA, USA) and NF-κB p65 (1:500, #3034, Cell Signaling). Signals were detected using corresponding horseradish peroxidase-conjugated secondary antibodies (1:5000, #NA934V, NA9310V, GE Healthcare Ltd., Great North Road Hatfield, UK) and enhanced chemiluminescence (#34095, Thermo Fisher, Waltham, MA,

Table 1 Primers list for qRT-PCR

Gene	Primer
18s-F	5′-ACGGAAGGGCACCACCAGGA-3′
18s-R	5′-CACCACCACCCACGGAATCG-3′
Il-6-F	5′-TAGTCCTTCCTACCCCAATTTCC-3′
Il-6-R	5′-TTGGTCCTTAGCCACTCCTTC-3′
Il-1β-F	5′- TTCAGGCAGGCAGTATCACTC-3′
Il-1β-R	5′-GAAGGTCCACGGGAAAGACAC-3′
Tnf-α-F	5′-CATCTTCTCAAAATTCGAGTGACAA-3′
Tnf-α-R	5′-TGGGAGTAGACAAGGTACAACCC-3′
Vegfa-F	5′-GGAGACTCTTCGAGGAGCACTT-3′
Vegfa-R	5′-GGCGATTTAGCAGCAGATATAAGAA-3′
Ffar4-F	5′-GCCCAACCGCATAGGAGAAA-3′
Ffar4-R	5′-GTCTTGTTGGGACACTCGGA-3′
Nfκb-F	5′-GGAGAGTCTGACTCTCCCTGAGAA-3′
Nfκb-R	5′-CGATGGGTTCCGTCTTGGT-3′

USA). GAPDH (1:1000, sc-32233; Santa Cruz, Dallas, TX, USA) was used as an internal control.

Enzyme-linked immunosorbent assay (ELISA)

The retina, choroid, RPE complexes were isolated from the mice eyes (male and female) 7 days after photocoagulation. Two eyes were placed into 100 μL of lysis buffer supplemented with protease inhibitors and sonicated. The lysate was centrifuged at 13,000×g for 20 min at 4 °C, and the levels of IL-6 was determined with the mouse IL-6 ELISA kits (R&D Systems, Minneapolis, MN, USA) according to the manufacturer's protocols.

Ex vivo choroid-sprouting assay

Ex vivo choroid-sprouting assays were performed as previously described [25]. Briefly, choroid RPE complex ("choroid explants'') were dissected from eyes from three-week-old C57BL/6J, *Ffar4*$^{-/-}$ and *Ffar4*$^{+/+}$ mice, then the peripheral area of the complexes was cut into approximately 1×1 mm pieces. The explants were immediately embedded in 30 μL growth factor reduced Matrigel (#354230, BD Biosciences, San Jose, CA, USA) in 24-well tissue culture plates. The choroidal explants were grown in CSC complete medium (#420-500, Cell Systems, Kirkland, WA, USA) supplemented with growth factor Boost and 1% Penicillin/Streptomycin (#15142, GIBCO, Grand Island, NY, USA) at 37 °C with 5% CO_2. After 6 days of ex vivo culture, images of the choroid sprouting were recorded, and the sprouting area was quantified using Image J.

Statistical analysis

Animal data are presented as mean ± standard error (SE). Student's unpaired two-tailed *t* test and ANOVA with Tukey's multiple comparison test was used for comparison of results as specified in the figure legends (Prism v8.0; GraphPad Software, Inc., San Diego, CA, USA). Statistically significant difference was set at $p < 0.05$.
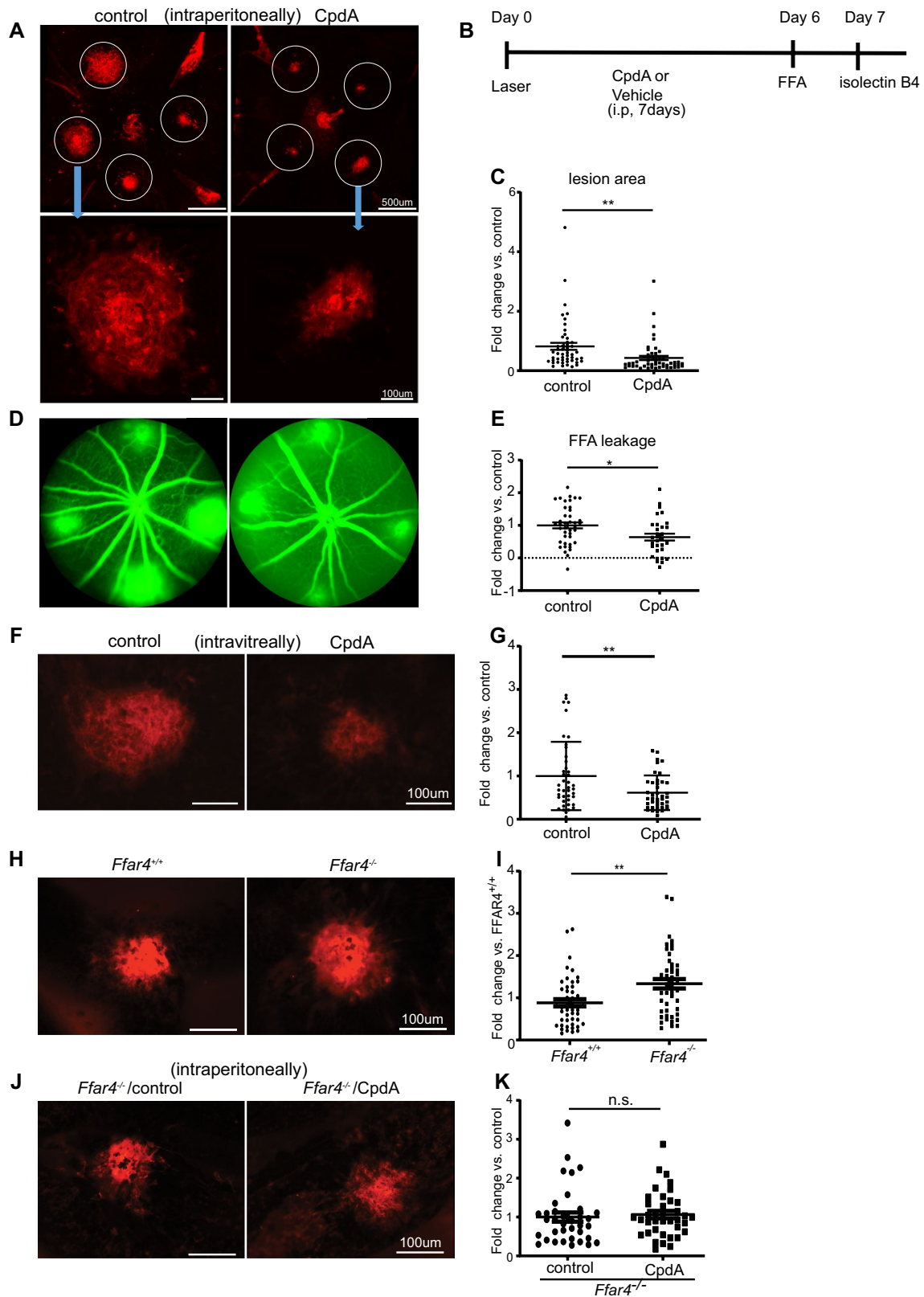
Results

FFAR4 agonist decreased lesion size and vascular leakage in the laser-induced CNV mouse model

To investigate the role of FFAR4 in CNV, we induced CNV by laser injury and treated mice with the FFAR4 agonist (CpdA, 30 mg/kg) or vehicle i.p. once a day from day 0 to day 6 and then quantified lesion size and vascular leakage at day 7 (Fig. 1a, b). CpdA treatment decreased lesion size by 47.3% at day 7 compared to the control group ($p = 0.004$)

(Fig. 1c). CpdA treatment decreased the intensity of vascular leakage by 36.1% compared to the control group ($p = 0.012$) (Fig. 1d, e).

To investigate whether CpdA affects the eye directly, we injected CpdA (50 μg/μl, 1 μl) or vehicle control into the vitreous humor immediately after laser photocoagulation.

◄**Fig. 1** FFAR4 activation decreased lesion size and leakage in the laser-induced CNV mouse model. **a** Representative retinal whole mount images of laser-induced vascular lesions (stained with red lectin) after intraperitoneal injection of vehicle control (left) or CpdA (right, FFAR4 agonist) at day 7. Scale bar = 500 μm (upper), 100 μm (lower). **b** The time course of the experiment **c** CpdA treatment decreased lesion size compared to control group ($n = 50$–52). **d** Representative whole mount laser-induced CNV images of control (left) and CpdA (right) treated retinas after fluorescein angiography at day 6. **e** CpdA decreased the intensity of vascular leakage compared to control ($n = 31$–41). **f** A representative image of laser-induced CNV lesion with intravitreal injection at day7. Left is the control. Right is CpdA treatment. **g** FFAR4 decreased lesion size compared to control ($n = 41$–42). scale bar = 100 μm **h** A representative image of laser-induced CNV lesion stained with red lectin in $Ffar4^{+/+}$ (left) and $Ffar4^{-/-}$ mice (right) at day 7. **i** $Ffar4^{-/-}$ increased laser-induced CNV lesion area ($n = 48$–49). **j** A representative image of laser-induced CNV lesion after i.p treatment with vehicle (left) and CpdA (right) in $Ffar4^{-/-}$ mice at day 7. **k** CpdA had no detectable effect on CNV lesion size in $Ffar4^{-/-}$ mice ($n = 36$–38). scale bars = 100 μm. The data were analyzed by Student's t-test and were expressed as mean ± SE. *$p < 0.05$; **$p < 0.01$; n.s. $p > 0.05$

Consistent with systemic administration of the CpdA, lesion size at day 7 was 38.5% decreased with intravitreal CpdA compared to the size in control group ($p = 0.007$) (Fig. 1f, g).

$Ffar4^{-/-}$ mice had larger laser-induced CNV lesions

To further examine whether FFAR4 influences the development of CNV in vivo, we laser-induced CNV in $Ffar4^{+/+}$ and $Ffar4^{-/-}$ littermate mice (male and female) at 6–8 weeks of age and compared lesions 7 days later. The values of neovascularization area before normalizing with littermate control were 12,731 μm^2 for $Ffar4^{-/-}$ and 8735 μm^2 for $Ffar4^{+/+}$ (Fig. 1h). $Ffar4^{-/-}$ mice had 45.0% increase in CNV lesion area compared to $Ffar4^{+/+}$ ($p = 0.013$) (Fig. 1i).

To address whether the CpdA acted specifically through FFAR4 and to exclude any off target effect, we injected CpdA (30 mg/kg) or vehicle (control) i.p. daily from day 0 to day 6 after CNV laser induction to $Ffar4^{-/-}$ littermate mice and evaluated lesions 7 days later. CpdA had no effect on CNV in $Ffar4^{-/-}$ mice ($p = 0.68$) (Fig. 1j, k).

FFAR4 agonist suppressed inflammation in the retina, choroid, RPE complex of mice with laser-induced CNV

To address the mechanism of FFAR4 agonism on CNV suppression, we focused on inflammation which is known to play an important role in CNV and because FFAR4 agonism has been previously shown to have robust anti-inflammatory effects [20, 22]. First, we measured the protein level of pNF-κB and NF-κB via immunoblot analysis in the retina, choroid, RPE complex of normal and laser-induced CNV mice with and without CpdA treatment (Fig. 2a). The ratio of pNF-κB to NF-κB in control was higher than in CpdA-treated

mice; that is the CpdA reduced the ratio compared to that in the control eye ($p = 0.004$) (Fig. 2b).

To investigate inflammation downstream of the NF-κB pathway, we measured mRNA expression of Tnf-α, Il-6, Il-1β, and $Vegfa$ in the retina, choroid, RPE complex of laser-induced mice with and without CpdA treatment using qRT-PCR analysis. CpdA reduced mRNA levels of major inflammation markers Il-6 and Il-1β compared to control ($p = 0.01$, 0.03, respectively) (Fig. 2c). CpdA also reduced protein levels of IL-6 with Sandwich ELISA compared to control in the retina, choroid, RPE complex of laser-induced mice ($n = 10$, male = 5, female = 5, $p = 0.037$, data not shown). Although there were no significant changes between two groups in Tnf-α, and $Vegfa$, CpdA tended to decrease Tnf-α. In contrast, CpdA did not influence inflammation markers in isolated retina (Fig. 2d). We confirmed that $Ffar4$ is expressed in the retina, choroid, RPE complex (Fig. 2e). We also examined the mRNA expression level of inflammation markers in laser-induced CNV in $Ffar4^{-/-}$ and $Ffar4^{+/+}$ mice. $Ffar4^{-/-}$ mice had increased Il-6 mRNA levels in the retina, choroid, RPE complex compared to $Ffar4^{+/+}$ mice ($p = 0.04$) (Fig. 2f).

FFAR4 suppressed inflammation in RPE cells

We isolated RPE from $Ffar4^{-/-}$ and $Ffar4^{+/+}$ littermate controls and confirmed the expression of $Ffar4$ in the RPE in the $Ffar4^{+/+}$ mice and the lack of expression in $Ffar4^{-/-}$ mice (Fig. 2g). We assessed the mRNA expression level of inflammation markers Tnf-α, Il-6, Il-1β and Nf-κb. All four markers (Tnf-α, Il-6, Il-1β, and Nf-κb) were increased in the primary RPE cells of $Ffar4^{-/-}$ mice compared with $Ffar4^{+/+}$ mice ($p = 0.04$, 0.04 and 0.003 respectively) (Fig. 2h).

FFAR4 agonist suppressed CNV ex vivo

We also evaluated the effects of loss of FFAR4 or the use of CpdA treatment on choroidal vascular sprouting using ex vivo choroid-sprouting assays, without retina present. Pieces of sclera and choroid with attached RPE were dissected from C57BL/6J, $Ffar4^{-/-}$ and $Ffar4^{+/+}$ littermate mice and cultured as previously described [25]. The sprouting area in $Ffar4^{+/+}$ explants showed significantly less vascular growth compared with $Ffar4^{-/-}$ explants at day 6 ($p = 0.004$) (Fig. 3a, b). Compared to untreated explants, CpdA treatment (1 μM) significantly reduced the choroidal sprouting from C57BL/6J mice at day 6 ($p = 0.03$) (Fig. 3c, d).

Discussion

We studied the influence of FFAR4 on CNV in an animal model. An FFAR4 agonist (CpdA) decreased the area of CNV compared to control. $Ffar4^{-/-}$ mice showed larger

Fig. 2 CpdA treatment in mice with laser-induced CNV decreased markers of inflammation. **a** Representative image of Western blotting analysis of pNF-κB and NF-κB expression in the retina, choroid, RPE complex. **b** Western blotting quantification: ratio of pNF-κB to NF-κB. The data were presented as the mean ± SE ($n = 5$–6). **c** Quantitative (q) RT-PCR analysis of *Tnf-α*, *Il-6*, *Il-1β*, and *Vegfa* mRNA expression levels in control vs CpdA treatment ($n = 6$–8). The samples are both retina, choroid, RPE complex. **d** qRT-PCR analysis of *Tnf-α*, *Il-6*, and *Il-1β* mRNA expression level in control vs CpdA treatment in the retina ($n = 3,4$). **e** FFAR4 mRNA expression level in the retina, choroid, RPE complex in *Ffar4*$^{+/+}$ vs *Ffar4*$^{-/-}$ ($n = 6$). **f** qRT-PCR analysis of *Tnf-α*, *Il-6*, *Il-1B*, and *Vegfa* mRNA expression level in *Ffar4*$^{+/+}$ vs *Ffar4*$^{-/-}$ ($n = 7$–9). **g** qRT-PCR analysis of *Ffar4* mRNA expression level between *Ffar4*$^{+/+}$ vs *Ffar4*$^{-/-}$ littermate mice ($n = 4$, pooled RPE per group) in the primary RPE. **h** qRT-PCR analysis of *Tnf-α*, *Il-6*, *Il-1β* and *Nf-κb* mRNA expression level in *Ffar4*$^{+/+}$ vs *Ffar4*$^{-/-}$ in the primary RPE ($n = 4$, pooled RPE per group). The data were analyzed by Student's t-test or ANOVA with Tukey's multiple comparison test and were expressed as mean ± SE. *$p < 0.05$; **$p < 0.01$; ****$p < 0.0001$; n.s. $p > 0.05$
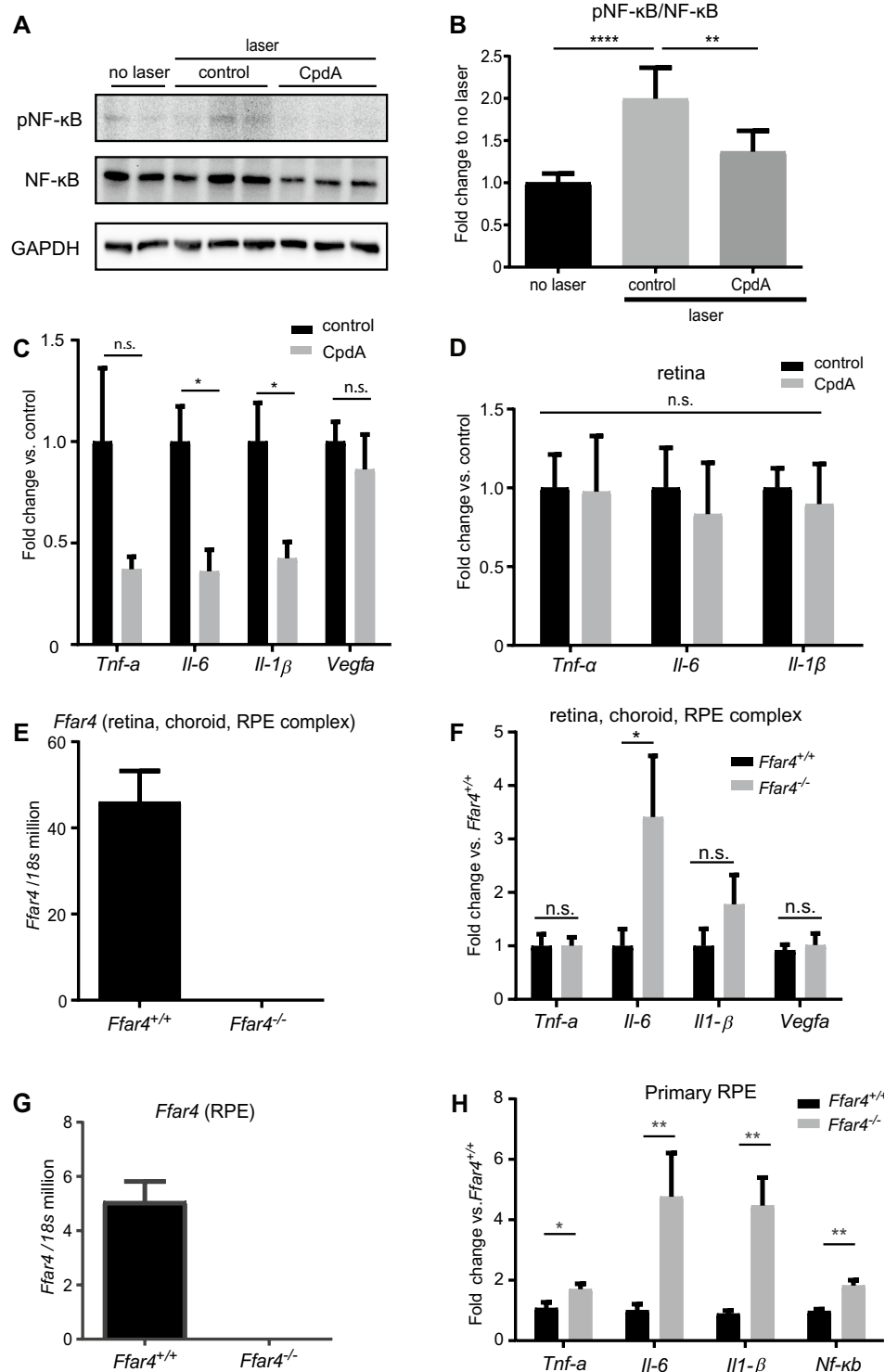
CNV areas after laser injury than *Ffar4*$^{+/+}$ mice. We confirmed that the effect of the FFAR4 agonist was mediated through FFAR4 (Fig. 1). Activation of FFAR4 by a small-molecule agonist downregulated NF-κB and decreased proinflammatory pathways (Fig. 2). Additionally, we found that FFAR4 activation suppressed neovascularization in

the ex vivo choroid-sprouting assay (Fig. 3). To further identify the cell type primarily involved in the suppression of CNV we focused on RPE for the following reasons. First, inflammation markers were specifically increased in the choroid RPE complex and not in retina alone. Second, the choroid-sprouting assay without retina but with
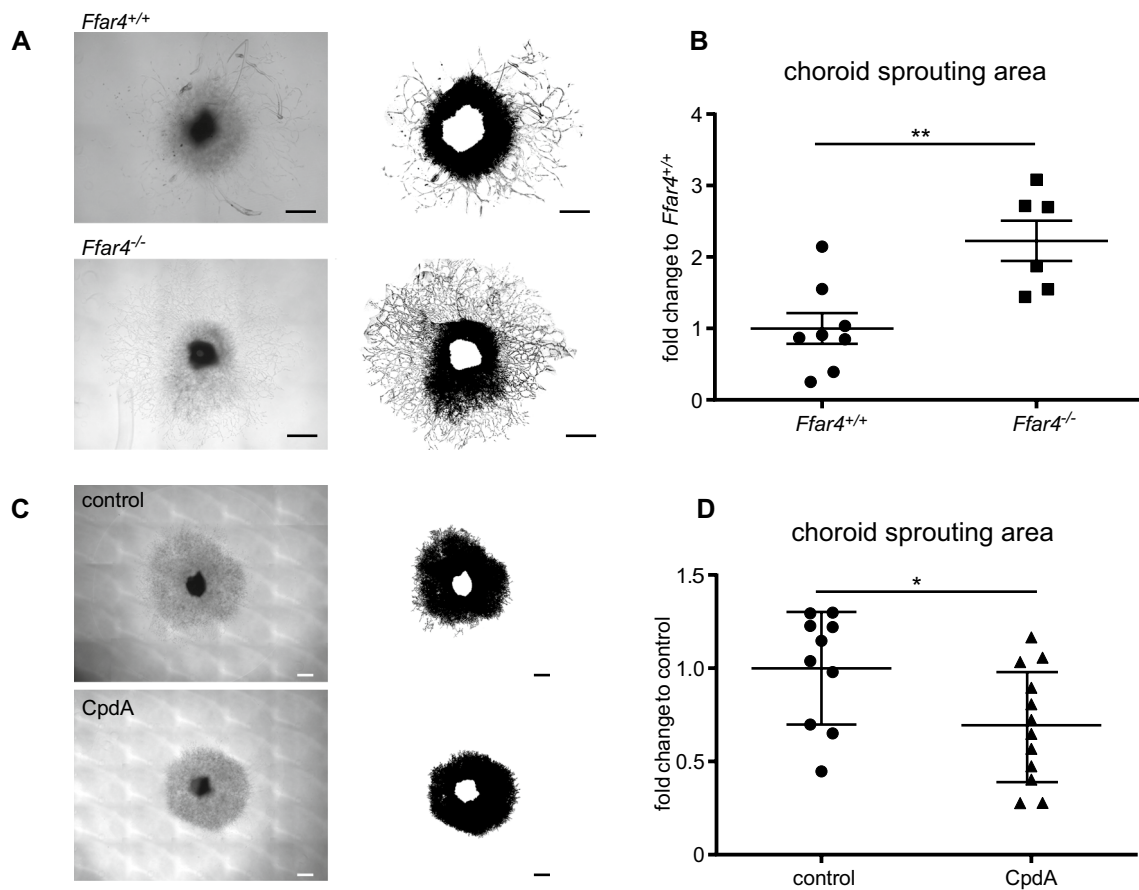
Fig. 3 CpdA suppressed choroidal neovascularization. **a** Representative images of the sprouting assay with choroid from *Ffar4*⁺/⁺ vs *Ffar4*⁻/⁻ mice: upper image is the choroid of *Ffar4*⁺/⁺, lower image is *Ffar4*⁻/⁻ choroid. **b** Choroid sprouting is increased in *Ffar4*⁻/⁻ vs *Ffar4*⁺/⁺ mice ($n = 6–8$). **c** Representative images of choroid sprouting: upper image shows vehicle treatment (control); lower image shows CpdA treatment. **d** CpdA suppressed choroidal sprouting compared to control ($n = 10–12$). Scale bars $= 500$ μm. The data were analyzed by Student's t-test and were expressed as mean $\pm$ SE. *$p < 0.05$; **$p < 0.01$

RPE showed decreased sprouting when treated with the FFAR4 agonist. Third, without RPE, the choroid complex will not sprout under assay conditions, suggesting that RPE is required for choroidal sprouting. Fourth, we confirmed that FFAR4 is present in RPE. In isolated RPE from *Ffar4*⁻/⁻ mice, the expression levels of *Il-6, Il-1β, Tnf-α, and Nfκb* were increased compared to *Ffar4*⁺/⁺ mice, consistent with our in vivo study. Taken together, these results suggest that RPE is involved in the inflammation pathway. Therefore, FFAR4 may suppress CNV by suppressing inflammation signaling in the RPE although other cell types may also be involved.

A previous study showed that the RPE and choroid are involved in neovascularization [25]. Others have also shown that RPE integrity is critical to CNV formation. When the RPE is damaged before or at the time of laser coagulation, CNV does not form [26]. We confirmed that *Ffar4* is expressed in RPE as previous study reported [18]. We also showed that FFAR4 influenced ex vivo choroid sprouting

(without retina present). FFAR4 agonist did not influence inflammation markers in the retina, only in RPE (Fig. 2).

Several groups have shown that activated FFAR4 recruits, binds and internalizes β-arrestin2 protein [20, 22]. β-arrestin-2 inhibits the activation of NF-κB, thereby promoting anti-inflammatory effects in several cells such as macrophages and adipocytes [20, 27, 28]. A group showed that FFA4 agonism by Docosahexaenoic acid (DHA) inhibits NLRP3 inflammasome activity, inhibits NF-κB, and reduces proinflammatory IL-1β production, in a manner dependent on β-arrestin-2 signaling [29]. Others showed that toll-like receptor 4 (TLR4) signaling through NF-κB, is inhibited by activation of FFAR4 in a β-arrestin-2-dependent manner [30]. FFAR4 could be also involved in NF-κB signaling via β-arrestin-2 in the RPE.

In CNV membranes from AMD patients, IL-1β is secreted by RPE and is a possible pro-angiogenic mediator in AMD [31]. IL-1 β induces vascular sprouting in aortic rings where sprouting is inhibited by IL-1R antagonist.

Fig. 4 Conceptual summary of proposed pathways. Schema of the FFAR4 pathway in mediating NF-κB inhibition of laser-induced CNV in RPE
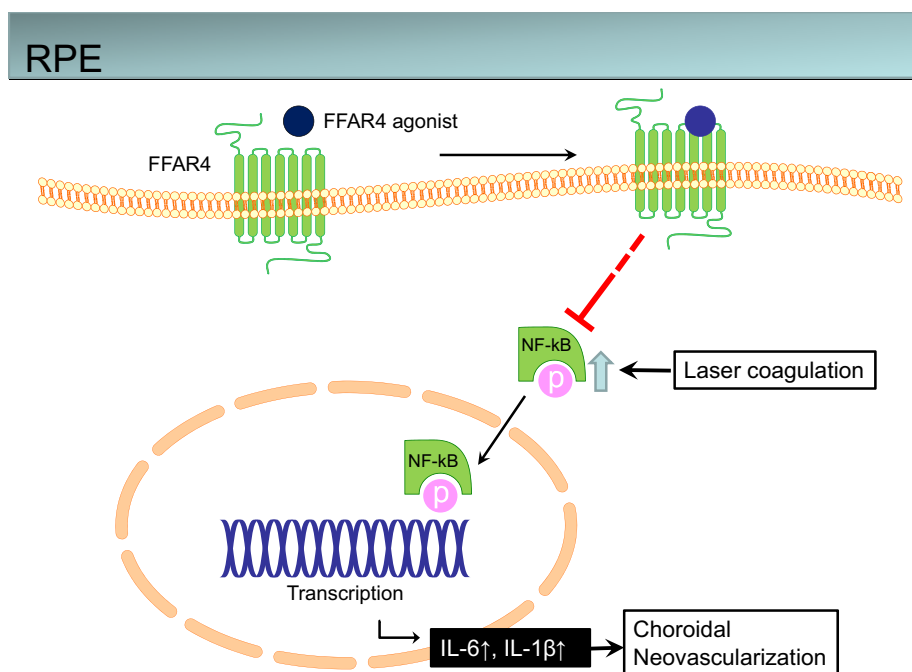
Thus, inflammation might be involved in vascular sprouting [32]. IL-6 levels in aqueous humor correlate with CNV size and macular thickness in patients with AMD [33, 34]. Another study indicates that CNV is suppressed by IL-6 receptor blockade in the laser-induced CNV model [35]. Our study also suggests that the effect of FFAR4 on CNV is independent of *Vegfa* (Fig. 2c, f). Taken together, our results suggest that in laser-induced CNV, FFAR agonist inhibits IL-6 and IL-1β via inhibiting NF-κB signaling in RPE cells to suppress CNV.

FFAR4 activation in primary adipose tissue and 3T3-L1 adipocytes leads to an increase in glucose transport and translocation of GLUT4 to the plasma membrane [28]. FFAR4 activation stimulates GLUT1 production [36]. Furthermore, FFAR4 activation stimulates β-oxidation in brown adipocytes [37]. However, in the laser-induced CNV model, FFAR4 did not influence GLUT1, GLUT4, or markers of β-oxidation (data not shown).

Several groups have suggested that omega-3 fatty acids prevent nonalcoholic fatty liver disease (NAFLD) and nonalcoholic steatohepatitis (NASH) via FFAR4 activation [22, 38–40]. FFAR4 may also be a potential target for the treatment of type 2 diabetes and obesity [41]. In addition, a FFAR4 agonist is in an ongoing clinical trial for type 2 diabetes and obesity. If it is approved as an anti-diabetic drug, a FFAR4 agonist could be repurposed as an anti-neovascular AMD drug.

In summary, we found that an FFAR4 agonist suppressed inflammation via the NF-κB pathway in laser-induced CNV via FFAR4 (Fig. 4) and suppressed CNV.

This is the first study of the relationship between FFAR4 and CNV in an animal model of CNV seen in neovascular AMD. Our results suggest FFAR4 to be a new molecular target to reduce pathological angiogenesis in AMD patients.

Compliance with ethical standards

Ethical approval All animal studies adhered to the Association for Research in Vision and Ophthalmology Statement for the Use of Animals in Ophthalmic and Vision Research and were approved by Institutional Animal Care and Use Committee at Boston Children's Hospital (ARCH Protocol Number 19-04-3913R).

References

1. Friedman DS, Ocolmain BJ, Munoz B, Tomany SC, McCarty C, de Jong PT, Nemesure B, Mitchell P, Kempen J, Eye Diseases Prevalence Research G (2004) Prevalence of age-related macular degeneration in the United States. Arch Ophthalmol 122(4):564–572. https://doi.org/10.1001/archopht.122.4.564

2. de Jong PT (2006) Age-related macular degeneration. N Engl J Med 355(14):1474–1485. https://doi.org/10.1056/NEJMra062326

3. Fintak DR, Shah GK, Blinder KJ, Regillo CD, Pollack J, Heier JS, Hollands H, Sharma S (2008) Incidence of endophthalmitis related to intravitreal injection of bevacizumab and ranibizumab. Retina 28(10):1395–1399. https://doi.org/10.1097/IAE.0b013e3181884fd2

4. Rasmussen A, Bloch SB, Fuchs J, Hansen LH, Larsen M, LaCour M, Lund-Andersen H, Sander B (2013) A 4-year longitudinal study of 555 patients treated with ranibizumab for neovascular age-related macular degeneration. Ophthalmology 120(12):2630–2636. https://doi.org/10.1016/j.ophtha.2013.05.018

5. Grunwald JE, Daniel E, Huang J, Ying GS, Maguire MG, Toth CA, Jaffe GJ, Fine SL, Blodi B, Klein ML, Martin AA, Hagstrom SA, Martin DF, Group CR (2014) Risk of geographic atrophy in the comparison of age-related macular degeneration treatments trials. Ophthalmology 121(1):150–161. https://doi.org/10.1016/j.ophtha.2013.08.015

6. Wong WL, Su X, Li X, Cheung CM, Klein R, Cheng CY, Wong TY (2014) Global prevalence of age-related macular degeneration and disease burden projection for 2020 and 2040: a systematic review and meta-analysis. Lancet Glob Health 2(2):e106–116. https://doi.org/10.1016/S2214-109X(13)70145-1

7. Lambert V, Lecomte J, Hansen S, Blacher S, Gonzalez ML, Struman I, Sounni NE, Rozet E, de Tullio P, Foidart JM, Rakic JM, Noel A (2013) Laser-induced choroidal neovascularization model to study age-related macular degeneration in mice. Nat Protoc 8(11):2197–2211. https://doi.org/10.1038/nprot.2013.135

8. Ryan SJ (1979) The development of an experimental model of subretinal neovascularization in disciform macular degeneration. Trans Am Ophthalmol Soc 77:707–745

9. Gong Y, Li J, Sun Y, Fu Z, Liu CH, Evans L, Tian K, Saba N, Fredrick T, Morss P, Chen J, Smith LE (2015) Optimization of an image-guided laser-induced choroidal neovascularization model in mice. PLoS ONE 10(7):e0132643. https://doi.org/10.1371/journal.pone.0132643

10. Saishin Y, Saishin Y, Takahashi K, Lima e Silva R, Hylton D, Rudge JS, Wiegand SJ, Campochiaro PA (2003) VEGF-TRAP(R1R2) suppresses choroidal neovascularization and VEGF-induced breakdown of the blood-retinal barrier. J Cell Physiol 195(2):241–248. https://doi.org/10.1002/jcp.10246

11. Noel A, Jost M, Lambert V, Lecomte J, Rakic JM (2007) Antiangiogenic therapy of exudative age-related macular degeneration: current progress and emerging concepts. Trends Mol Med 13(8):345–352. https://doi.org/10.1016/j.molmed.2007.06.005

12. Fu Z, Chen CT, Cagnone G, Heckel E, Sun Y, Cakir B, Tomita Y, Huang S, Li Q, Britton W, Cho SS, Kern TS, Hellstrom A, Joyal JS, Smith LE (2019) Dyslipidemia in retinal metabolic disorders. EMBO Mol Med 11(10):e10473. https://doi.org/10.15252/emmm.201910473

13. Yasukawa T, Wiedemann P, Hoffmann S, Kacza J, Eichler W, Wang YS, Nishiwaki A, Seeger J, Ogura Y (2007) Glycoxidized particles mimic lipofuscin accumulation in aging eyes: a new age-related macular degeneration model in rabbits. Graefes Arch Clin Exp Ophthalmol 245(10):1475–1485. https://doi.org/10.1007/s00417-007-0571-z

14. Yasukawa T (2009) Inflammation in age related macular degeneration: pathological or physiological? Expert Rev Ophthalmol 4(2):107–112

15. Connor KM, SanGiovanni JP, Lofqvist C, Aderman CM, Chen J, Higuchi A, Hong S, Pravda EA, Majchrzak S, Carper D, Hellstrom A, Kang JX, Chew EY, Salem N Jr, Serhan CN, Smith LEH (2007) Increased dietary intake of omega-3-polyunsaturated fatty acids reduces pathological retinal angiogenesis. Nat Med 13(7):868–873. https://doi.org/10.1038/nm1591

16. Joyal JS, Sun Y, Gantner ML, Shao Z, Evans LP, Saba N, Fredrick T, Burnim S, Kim JS, Patel G, Juan AM, Hurst CG, Hatton CJ, Cui Z, Pierce KA, Bherer P, Aguilar E, Powner MB, Vevis K, Boisvert M, Fu Z, Levy E, Fruttiger M, Packard A, Rezende FA, Maranda B, Sapieha P, Chen J, Friedlander M, Clish CB, Smith LE (2016) Retinal lipid and glucose metabolism dictates angiogenesis through the lipid sensor Ffar1. Nat Med 22(4):439–445. https://doi.org/10.1038/nm.4059

17. Ulven T, Christiansen E (2015) Dietary fatty acids and their potential for controlling metabolic diseases through activation of FFA4/GPR120. Annu Rev Nutr 35:239–263. https://doi.org/10.1146/annurev-nutr-071714-034410

18. Datilo MN, Sant'Ana MR, Formigari GP, Rodrigues PB, de Moura LP, da Silva ASR, Ropelle ER, Pauli JR, Cintra DE (2018) Omega-3 from flaxseed oil protects obese mice against diabetic retinopathy through GPR120 receptor. Sci Rep 8(1):14318. https://doi.org/10.1038/s41598-018-32553-5

19. Ichimura A, Hirasawa A, Poulain-Godefroy O, Bonnefond A, Hara T, Yengo L, Kimura I, Leloire A, Liu N, Iida K, Choquet H, Besnard P, Lecoeur C, Vivequin S, Ayukawa K, Takeuchi M, Ozawa K, Tauber M, Maffeis C, Morandi A, Buzzetti R, Elliott P, Pouta A, Jarvelin MR, Korner A, Kiess W, Pigeyre M, Caiazzo R, Van Hul W, Van Gaal L, Horber F, Balkau B, Levy-Marchal C, Rouskas K, Kouvatsi A, Hebebrand J, Hinney A, Scherag A, Pattou F, Meyre D, Koshimizu TA, Wolowczuk I, Tsujimoto G, Froguel P (2012) Dysfunction of lipid sensor GPR120 leads to obesity in both mouse and human. Nature 483(7389):350–354. https://doi.org/10.1038/nature10798

20. Oh DY, Talukdar S, Bae EJ, Imamura T, Morinaga H, Fan W, Li P, Lu WJ, Watkins SM, Olefsky JM (2010) GPR120 is an omega-3 fatty acid receptor mediating potent anti-inflammatory and insulin-sensitizing effects. Cell 142(5):687–698. https://doi.org/10.1016/j.cell.2010.07.041

21. Janssen S, Laermans J, Iwakura H, Tack J, Depoortere I (2012) Sensing of fatty acids for octanoylation of ghrelin involves a gustatory G-protein. PLoS ONE 7(6):e40168. https://doi.org/10.1371/journal.pone.0040168

22. Oh DY, Walenta E, Akiyama TE, Lagakos WS, Lackey D, Pessentheiner AR, Sasik R, Hah N, Chi TJ, Cox JM, Powels MA, Di Salvo J, Sinz C, Watkins SM, Armando AM, Chung H, Evans RM, Quehenberger O, McNelis J, Bogner-Strauss JG, Olefsky JM (2014) A Gpr120-selective agonist improves insulin resistance and chronic inflammation in obese mice. Nat Med 20(8):942–947. https://doi.org/10.1038/nm.3614

23. Fu Z, Liegl R, Wang Z, Gong Y, Liu CH, Sun Y, Cakir B, Burnim SB, Meng SS, Lofqvist C, SanGiovanni JP, Hellstrom A, Smith LEH (2017) Adiponectin mediates dietary omega-3 long-chain polyunsaturated fatty acid protection against choroidal neovascularization in mice. Invest Ophthalmol Vis Sci 58(10):3862–3870. https://doi.org/10.1167/iovs.17-21796

24. Xin-Zhao Wang C, Zhang K, Aredo B, Lu H, Ufret-Vincenty RL (2012) Novel method for the rapid isolation of RPE cells specifically for RNA extraction and analysis. Exp Eye Res 102:1–9. https://doi.org/10.1016/j.exer.2012.06.003

25. Shao Z, Friedlander M, Hurst CG, Cui Z, Pei DT, Evans LP, Juan AM, Tahiri H, Duhamel F, Chen J, Sapieha P, Chemtob S, Joyal JS, Smith LE (2013) Choroid sprouting assay: an ex vivo model

of microvascular angiogenesis. PLoS ONE 8(7):e69552. https://doi.org/10.1371/journal.pone.0069552

26. Garcia-Layana A, Vasquez G, Salinas-Alaman A, Moreno-Montanes J, Recalde S, Fernandez-Robredo P (2009) Development of laser-induced choroidal neovascularization in rats after retinal damage by sodium iodate injection. Ophthal Res 42(4):205–212. https://doi.org/10.1159/000232946

27. Moniri NH (2016) Free-fatty acid receptor-4 (GPR120): Cellular and molecular function and its role in metabolic disorders. Biochem Pharmacol 110–111:1–15. https://doi.org/10.1016/j.bcp.2016.01.021

28. Talukdar S, Olefsky JM, Osborn O (2011) Targeting GPR120 and other fatty acid-sensing GPCRs ameliorates insulin resistance and inflammatory diseases. Trends Pharmacol Sci 32(9):543–550. https://doi.org/10.1016/j.tips.2011.04.004

29. Williams-Bey Y, Boularan C, Vural A, Huang NN, Hwang IY, Shan-Shi C, Kehrl JH (2014) Omega-3 free fatty acids suppress macrophage inflammasome activation by inhibiting NF-kappaB activation and enhancing autophagy. PLoS ONE 9(6):e97957. https://doi.org/10.1371/journal.pone.0097957

30. Li X, Yu Y, Funk CD (2013) Cyclooxygenase-2 induction in macrophages is modulated by docosahexaenoic acid via interactions with free fatty acid receptor 4 (FFA4). FASEB J 27(12):4987–4997. https://doi.org/10.1096/fj.13-235333

31. Oh H, Takagi H, Takagi C, Suzuma K, Otani A, Ishida K, Matsumura M, Ogura Y, Honda Y (1999) The potential angiogenic role of macrophages in the formation of choroidal neovascular membranes. Invest Ophthalmol Vis Sci 40(9):1891–1898

32. Lavalette S, Raoul W, Houssier M, Camelo S, Levy O, Calippe B, Jonet L, Behar-Cohen F, Chemtob S, Guillonneau X, Combadiere C, Sennlaub F (2011) Interleukin-1beta inhibition prevents choroidal neovascularization and does not exacerbate photoreceptor degeneration. Am J Pathol 178(5):2416–2423. https://doi.org/10.1016/j.ajpath.2011.01.013

33. Roh MI, Kim HS, Song JH, Lim JB, Koh HJ, Kwon OW (2009) Concentration of cytokines in the aqueous humor of patients with naive, recurrent and regressed CNV associated with amd after bevacizumab treatment. Retina 29(4):523–529. https://doi.org/10.1097/IAE.0b013e318195cb15

34. Miao H, Tao Y, Li XX (2012) Inflammatory cytokines in aqueous humor of patients with choroidal neovascularization. Mol Vis 18:574–580

35. Izumi-Nagai K, Nagai N, Ozawa Y, Mihara M, Ohsugi Y, Kurihara T, Koto T, Satofuka S, Inoue M, Tsubota K, Okano H, Oike Y, Ishida S (2007) Interleukin-6 receptor-mediated activation of signal transducer and activator of transcription-3 (STAT3) promotes choroidal neovascularization. Am J Pathol 170(6):2149–2158. https://doi.org/10.2353/ajpath.2007.061018

36. Huang J, Xue M, Zhang J, Yu H, Gu Y, Du M, Ye W, Wan B, Jin M, Zhang Y (2019) Protective role of GPR120 in the maintenance of pregnancy by promoting decidualization via regulation of glucose metabolism. EBioMedicine 39:540–551. https://doi.org/10.1016/j.ebiom.2018.12.019

37. Schilperoort M, van Dam AD, Hoeke G, Shabalina IG, Okolo A, Hanyaloglu AC, Dib LH, Mol IM, Caengprasath N, Chan YW, Damak S, Miller AR, Coskun T, Shimpukade B, Ulven T, Kooijman S, Rensen PC, Christian M (2018) The GPR120 agonist TUG-891 promotes metabolic health by stimulating mitochondrial respiration in brown fat. EMBO Mol Med. https://doi.org/10.15252/emmm.201708047

38. Nakamoto K, Tokuyama S (2019) Involvement of the free fatty acid receptor GPR120/FFAR4 in the development of nonalcoholic steatohepatitis. Yakugaku Zasshi 139(9):1169–1175. https://doi.org/10.1248/yakushi.19-00011-4

39. Nobili V, Carpino G, Alisi A, De Vito R, Franchitto A, Alpini G, Onori P, Gaudio E (2014) Role of docosahexaenoic acid treatment in improving liver histology in pediatric nonalcoholic fatty liver disease. PLoS ONE 9(2):e88005. https://doi.org/10.1371/journal.pone.0088005

40. Raptis DA, Limani P, Jang JH, Ungethum U, Tschuor C, Graf R, Humar B, Clavien PA (2014) GPR120 on Kupffer cells mediates hepatoprotective effects of omega3-fatty acids. J Hepatol 60(3):625–632. https://doi.org/10.1016/j.jhep.2013.11.006

41. Hudson BD, Shimpukade B, Mackenzie AE, Butcher AJ, Pediani JD, Christiansen E, Heathcote H, Tobin AB, Ulven T, Milligan G (2013) The pharmacology of TUG-891, a potent and selective agonist of the free fatty acid receptor 4 (FFA4/GPR120), demonstrates both potential opportunity and possible challenges to therapeutic agonism. Mol Pharmacol 84(5):710–725. https://doi.org/10.1124/mol.113.087783